LIMNOLOGY
and
OCEANOGRAPHY: METHODS

Limnol. Oceanogr.: Methods 11, 2013, 616–630

Inner filter correction of dissolved organic matter fluorescence

Dolly N. Kothawala[1], Kathleen R. Murphy[2], Colin A. Stedmon[3], Gesa A. Weyhenmeyer[1], and Lars J. Tranvik[1]*

[1]Department of Ecology and Genetics/Limnology, Evolutionary Biology Centre, Norbyvägen 18D, Uppsala University, Uppsala, Sweden, 75236

[2]Water Research Centre, The University of New South Wales, Sydney NSW 2052, Australia

[3]National Institute for Aquatic Resources, Section for Oceanography and Climate, Technical University of Denmark, Kavalergården 6, DK-2920, Charlottenlund, Denmark

Abstract

The fluorescence of dissolved organic matter (DOM) is suppressed by a phenomenon of self-quenching known as the inner filter effect (IFE). Despite widespread use of fluorescence to characterize DOM in surface waters, the advantages and constraints of IFE correction are poorly defined. We assessed the effectiveness of a commonly used absorbance-based approach (ABA), and a recently proposed controlled dilution approach (CDA) to correct for IFE. Linearity between corrected fluorescence and total absorbance (A_{Total}; the sum of absorbance at excitation and emission wavelengths) across the full excitation-emission matrix (EEM) in dilution series of four samples indicated both ABA and CDA were effective to an absorbance of at least 1.5 in a 1 cm cell, regardless of wavelength positioning. In regions of the EEMs where signal to background noise (S/N) was low, CDA correction resulted in more variability than ABA correction. From the ABA algorithm, the onset of significant IFE (>5%) occurs when absorbance exceeds 0.042. In these cases, IFE correction is required, which was the case for the vast majority (97%) of lakes in a nationwide survey (n= 554). For highly absorbing samples, undesirably large dilution factors would be necessary to reduce absorbance below 0.042. For rare EEMs with $A_{Total} > 1.5$ (3.0% of the lakes in the Swedish survey), a 2-fold dilution is recommended followed by ABA or CDA correction. This study shows that for the vast majority of natural DOM samples the most commonly applied ABA algorithm provides adequate correction without prior dilution.

The optical properties of dissolved organic matter (DOM) can yield valuable insights into its origin and biogeochemical function (Coble et al. 1990), and are studied widely across scientific disciplines including freshwater, marine, and soil sciences (Fellman et al. 2010). Fluorescence spectroscopy is also a particularly attractive monitoring tool in the water industry for sewage effluent (Baker et al. 2004), or for tracking changes in source water for drinking water utilities (Henderson et al. 2009; Hudson et al. 2007). Fluorescence measurements in samples with high absorbance are common for surface waters, however, their accurate measurement is dependent on accounting for inner filter effects (IFE) (Lakowicz 2006). Despite recent efforts to standardize measurement of fluorescence excitation-emission matrixes (EEM) for DOM (Murphy et al. 2010), advice regarding the treatment of IFE is incomplete and inconsistent, such that the efficacy and limitations of commonly used, and proposed, IFE correction methods remains unclear.

DOM contains a complex mixture of fluorophores which fluoresce over a wide range of wavelengths, displaying several characteristic peaks (Fig. 1a) (Coble 1996). Fluorescence intensity increases linearly with absorbance or concentration up to a threshold at which the fluorescence signal becomes suppressed by IFE due to the absorption of excitation and emission light within the cuvette. IFE can be segregated into primary IFE resulting from the attenuation of the excitation light, and secondary IFE attenuating the fluorescence (Fig. 1b). The total attenuation of fluorescence due to IFE at each wavelength pair across an EEM is a function of absorbance at the respective wavelengths and the pathlength. Since the absorbance spectrum of DOM decreases approximately expo-

*Corresponding author: E-mail: dolly.kothawala@ebc.uu.se

Acknowledgments:

The first two co-authors (DNK and KRM) contributed equally to this manuscript. We thank Jan Johansson and Xing Ji for technical support with optical analysis. We thank the Swedish Environmental Protection Agency, and the Department of Aquatic Sciences and Assessment at the Agricultural University of Sweden, particularly Christian Demandt and Jens Fölster for support with chemistry analyses and lake sampling. We thank the Swedish Research Council for Environment, Agricultural Sciences and Spatial Planning (FORMAS) for funding the strong research environments project called, The Color of Water. KRM acknowledges Australian Research Council funding for DP1096691.

DOI 10.4319/lom.2013.11.616

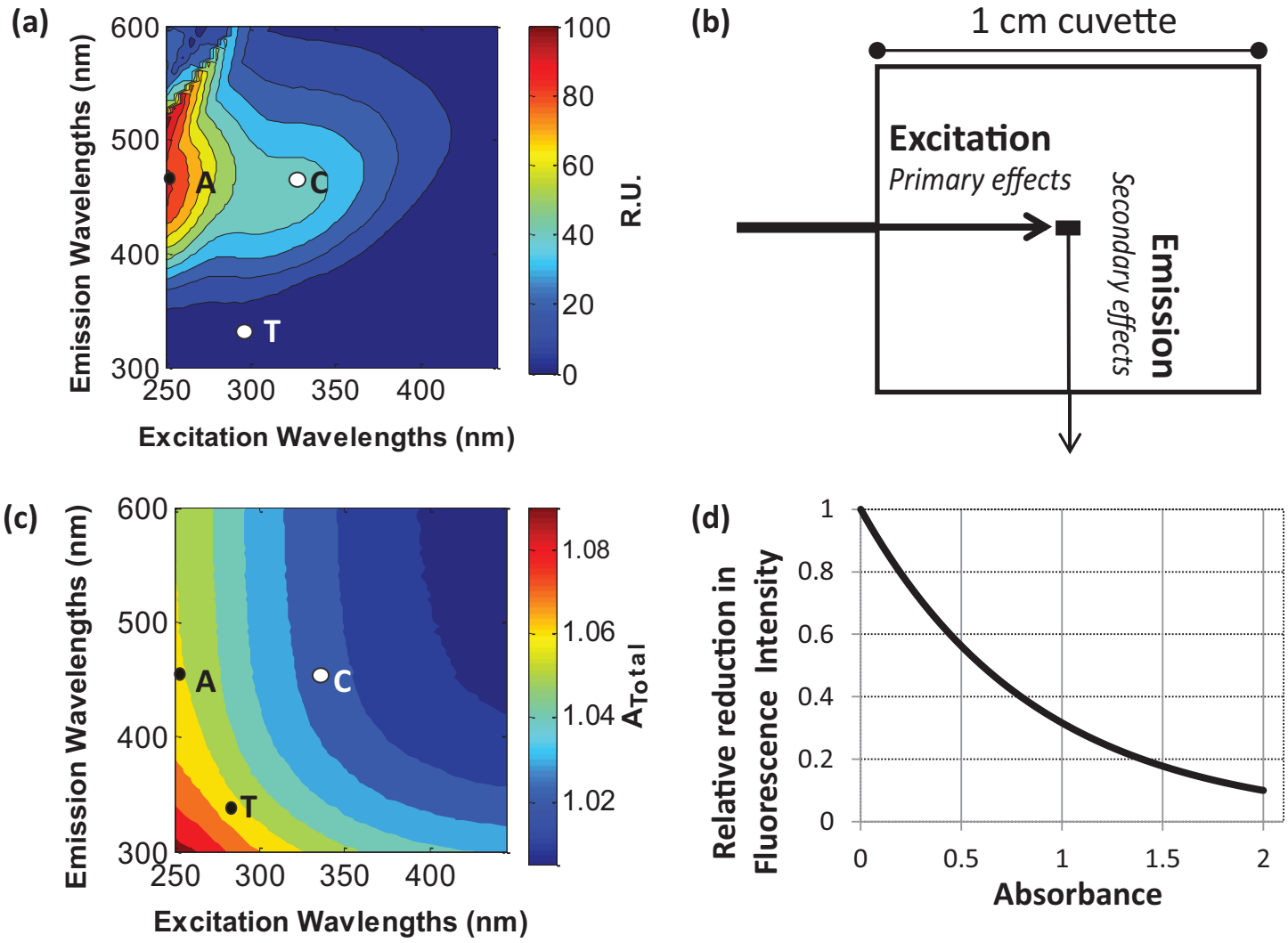

Fig. 1. (a) Example of an EEM for a concentrated lake water sample. (b) Schematic of the attenuation of light energy attributed to primary and secondary IFE in a 1 cm cuvette during fluorescence analysis; (c) example of the distribution of IFE across an EEM of dissolved organic matter, with the intensity scale expressing the sum of absorbance at any reference excitation-emission wavelength pair (A_{Total}), and identifying commonly referenced Peaks A, C, and T on the EEM. (d) Relative loss in fluorescence intensity due to IFE as a function of increasing A_{Total} (see absorbance-based correction Eq.1), which is valid for all excitation-emission wavelength pairs ($\lambda_{ex}/\lambda_{em}$) used to calculate A_{Total} based on measurements in a 1 cm cuvette.

nentially with increasing wavelength, IFE are most severe at shorter wavelengths, and particularly affect the transmission of excitation light (Fig. 1c); this alters the shape and positioning of fluorescence spectra resulting in a shift toward longer emission wavelengths (red-shifting) with increasing DOM concentrations (Mobed et al. 1996). The attenuation of fluorescence attributed to IFE can be easily estimated from the absorbance spectrum of the same sample (Fig. 1d).

Most fluorescence spectrophotometers used to measure DOM in environmental samples today employ a fixed 90° degree angle between excitation and emission light paths and a standard 1 cm quartz cuvette cell, in which IFE are significant even at low analyte concentrations. For this instrument configuration, the most commonly used method to correct DOM fluorescence spectra for IFE is the ABA, whereby IFE are estimated from an absorbance measurement and removed algebraically (Holland et al. 1977; Lakowicz 2006; Miller 1981). The CDA is a more recently proposed method that corrects for IFE using the fluorescence measurement of an additional diluted sample, without need for absorbance spectra (Luciani et al. 2009). Other approaches have been proposed including the Raman Scatter Approach (Larsson et al. 2007) which uses measurements of the Raman water peak to correct for IFE. However, for most surface water samples, the Raman water peak is engulfed by DOM fluorescence, limiting the applicability of this approach to extremely low-concentration samples.

Previous studies examining the efficacy of ABA correction for pure fluorophores (Birdsall et al. 1983; Eftink 1997) have

reported the range of linearity between corrected fluorescence intensity and absorbance extends to an absorbance of 2.0 or above (Christmann et al. 1980; Gu and Kenny 2009; Holland et al. 1977). At higher absorbance, various sources of error, along with the sensitivity of instruments became limiting, and eventually too great to accurately correct using this algorithm.

Literature pertaining specifically to DOM fluorescence over the past decade indicates widespread confusion with respect to the effectiveness of IFE correction. First, the range of absorbance permitting effective ABA correction needs clarification. Many studies have adopted the criteria of Ohno (2002), who identified an upper threshold absorbance at 254 nm (A254) of 0.3 in a 1 cm cuvette for accurately correcting the humification index (HIX, a ratio of peak areas across an emission spectra [435-480 nm/300-345 nm], at a single excitation wavelength, 254 nm; Ohno 2002; Zsolnay et al. 1999). Samples with A254 above 0.3 would require an additional dilution step before implementing ABA correction. This upper threshold is not necessarily transferable to fluorescence intensity across the EEM. Samples from surface waters and soils commonly have an absorbance exceeding 0.3, thus, there is a pressing need to identify the true range of effective IFE corrections across the full fluorescence spectra of typical DOM samples. Second, there is a widespread misunderstanding about the lower absorbance limit below which samples are not significantly affected by IFE. In some cases, this has resulted in insufficient dilution being used as a substitute for IFE correction. A wide range of dissolved organic carbon (DOC) concentrations have been reported above which IFE begins to significantly suppress fluorescence intensity, spanning from 1 mg C L^{-1} (Westerhoff et al. 2001) up to 100 mg C L^{-1} (Senesi et al. 1991), as reviewed elsewhere (Hudson et al. 2007). This confusion is unnecessary since an unambiguous indication of the onset of IFE, in terms of a minimum absorbance, can be mathematically extracted from the ABA equation, as discussed below.

The aim of this study was to test the efficacy of two simple algebraic approaches, ABA and CDA, for correcting IFE in EEMs measured on a bench-top fluorometer with standard right-angle geometry. A universal absorbance threshold identifying when IFE begins to suppress fluorescence is identified from theoretical principles. We test and demonstrate the effectiveness of ABA and CDA correction approaches using dilution series constructed from four natural samples assessed across the full EEM. We further evaluate ABA using samples from 554 Swedish lakes spanning the range of absorbance typical of boreal lakes. A downloadable MATLAB model is developed to examine the sensitivity of IFE methods exposed to experimental and instrument error at varying EEM wavelengths. This study attempts to improve the overall understanding of IFE correction approaches and clarify misunderstandings regarding IFE on concentrated water samples so that fluorescence studies of DOM can be implemented in a robust and consistent manner.

Methods

Study sites

Spectral analysis was performed on four dilution series using samples from four systems: 1) lake water collected from Gäddtjärn (pH 6.1), a small shallow moderately humic lake with maximum depth of 10 m (15.2 mg DOC L^{-1}) surrounded by wetland and forest, located in south-central Sweden (59°54′ N 17° 08′ E), 2) A river called Färgeån (pH 6.2), located in south-central Sweden (63°16′ N 13° 36′ E) (24.0 mg DOC L^{-1}), 3) a concentrate prepared with reverse osmosis and by tangential flow ultrafiltration (Kragh et al. 2008) from Öreälven River (pH 6.8), in Northern Sweden (64° 10′ N 18° 55′) (original sample 69.9 mg DOC L^{-1}), and 4) Nordic Reservoir DOM (pH 6.0), an organic matter standard sourced from a drinking water reservoir in Vallsjøen, Skarnes, Norway and isolated by reverse osmosis (IHSS, www.humicsubstances.org/isolation.html). The Nordic standard was prepared by dissolving in Milli-Q water to a stock concentration of 69.9 mg DOC L^{-1}.

In addition to the dilution series, 554 samples from an extensive Lake Survey (2009 and 2010) across the full geographical gradient of Sweden were available from the Swedish national monitoring program. At each lake, one water sample was collected by helicopter from the mid-point of the lake at a depth of 0.5 m. Lakes were well-mixed during the sampling period (Sep–Nov). For more information on the national monitoring program including methods, see Swedish University of Agricultural Science, Department of Aquatic Sciences and Assessment (www.slu.se/vatten-miljo).

Sample preparation

Dilution series were prepared by diluting the original sample with Milli-Q water (pH ~5.7) gravimetrically using glassware that had been acid washed and muffled at 450°C for 4 h. Dilutions were prepared for Gäddtjärn (n = 22), Färgeån (n = 20), Öreälven River (n = 21), and Nordic (n = 36). Within each dilution series, two alternating series of dilution factors were selected along a base-2 scale, this created a multitude of 2 times dilution factors necessary for assessing the CDA (Section 2.9). We compared dilution factors that were calculated using i) gravimetric measurements, ii) DOC measurements, and iii) the integral of absorbance across wavelengths relevant to fluorescence (250 to 600 nm), which indicated that gravimetric and absorbance-based dilution factors (DF) were similarly reliable (Web Appendix, Supplemental Fig. 1), and more reliable than dilution factors based on DOC measurements. For consistency, gravimetrically determined dilution factors were used throughout the study.

All samples in the dilution series and the Lake Survey were filtered with 0.45 μm regenerated cellulose (RC) membrane syringe filters (Satorius Stedim Biotech) before spectral analysis. Samples in the dilution series were not acidified or buffered. All samples were filtered and analyzed up to a maximum of 10 days from collection. The pH of undiluted samples in this study spanned from 6.0 to 6.8. Variation in pH across

the dilution series was < 1 pH unit for all samples except Nordic, which spanned 1.2 pH units. Across this range of pH, changes in fluorescence intensities have been previously shown to be on the order of 5% (Peak A) or insignificant (Peak C) (Patel-Sorrentino et al. 2002).

DOC and chemical measurements

Dissolved organic carbon (DOC) concentration was determined for each sample in the dilution series using a portable Sievers 900 total organic carbon analyzer (General Electric Analytical Instruments) with an accuracy of ± 2%. Lake Survey samples were analyzed for total organic carbon (TOC), pH, nitrate (NO_3^-), calcium (Ca^{+2}), and other standard water chemistry variables in a certified laboratory, using standard methods within 2 weeks of collection (www.slu.se/sv/fakulteter/nl/om-fakulteten/institutioner/institutionen-for-vatten-och-miljo/laboratorier/vattenkemiska-laboratoriet/vattenkemiska-analysmetoder). Because we quantified organic matter based on carbon content, we refer to the concentration of organic matter as DOC. However, when referring to spectral properties throughout the manuscript we use the term DOM, since absorbance and fluorescence reflect molecular structures other than carbon.

Absorbance measurements

Absorbance spectra were measured from 250 to 600 nm at 1 nm intervals using a Lambda 40 UV-visible spectrophotometer (Perkin Elmer, Waltham, USA), in a 1 cm quartz cuvette with Milli-Q water used as the blank. This spectrophotometer had a maximum absorbance of 4.0, and an accuracy of 0.1 nm. We used a scan speed of 240 nm $min^{-1,}$ and a slit width of 2.0 nm. We report the decadal absorbance (A_λ) throughout this manuscript, which is the measurement obtained directly from the absorbance spectrophotometer across a path length of 1 cm, and is unitless ($\log_{10}$ of transmittance) (Braslavsky 2007).

Fluorescence measurements

Excitation-emission matrices (EEMs) were analyzed using a fluorescence spectrophotometer (SPEX FluoroMax-2, Horiba Jobin Yvon) with a 1 cm quartz cuvette, run in sample emission to lamp reference mode (S/R). The excitation wavelengths (λ_{ex}) spanned from 250 to 445 nm in 5 nm increments, and emission wavelengths (λ_{em}) from 300 to 600 nm in 4 nm increments. Excitation and emission slit widths were set to 5 nm, and the integration time was 0.1 s. EEMs were blank-subtracted using the EEM of Milli-Q water. To correct S/R readings for instrument specific biases pertaining to both excitation and emission wavelengths post analysis, manufacturer supplied correction factors were applied to convert S/R to the corrected S_c/R_c (Coble et al. 1993). EEMs were calibrated to Raman units (RU), by dividing by the Raman area of pure water integrated over a λ_{em} range of 381 to 426 nm, at an λ_{ex} of 350 nm (Lawaetz and Stedmon 2009; Murphy et al. 2010)

To visually compare changes to the intensity and shape of excitation spectra (at λ_{em} 448 nm) from a dilution series before (Fig. 2a) and after IFE corrections (Fig. 2b), fluorescence intensities were multiplied by the dilution factor and normalized by the integral of the area of the excitation spectra (λ_{ex} from 250 to 445 nm, at λ_{em} 448 nm). In the absence of IFE, spectra across a dilution series should lie directly on top of each other (Fig. 2b).

Limit of fluorescence reporting

The limit of reporting (LOR) is the smallest amount of analyte that can be quantified, in this case by fluorescence intensity, with a reasonable level of precision. LOR was calculated for the spectrofluorometer in this study from the standard deviation (SD) of 10 individual blank EEMs, according to Eq. 1.

$$\text{LOR } F_{(\lambda em,\ \lambda ex)} = F_{\text{blank}(\lambda em,\ \lambda ex)} + 10 \times SD(F_{\text{blank}(\lambda em,\ \lambda ex)}) \quad (1)$$

LOR in this study varied by over an order of magnitude across the EEM (Web Appendix, Supplemental Fig. 2), with the lowest LOR (highest S/N) in the Peak C region and highest LOR (lowest S/N) in the protein-like region including Peak T.

Defining absorbance as A_{Total}

The relationship between A_{Total} and DOC concentration was variable between dilution series, as were the range of absorbances and DOC concentrations used (Table 1). To define the extent of IFE and the effectiveness of correction approaches, we related fluorescence intensity to absorbance, rather than DOC concentration. For this reason, we define absorbance as the A_{Total} corresponding to any wavelength pair of interest ($\lambda_{ex}/\lambda_{em}$) on the EEM. The sum of absorbance at

Table 1. Relationships between the sum of absorbance at Peak A (A_{Total} at $\lambda_{ex}/\lambda_{em}$ = 250/448) and DOC concentrations for four dilution series (Gäddtjärn, Färgeån, Örälven, and Nordic Reservoir) and a nationwide Swedish Lake Survey, with the standard error (SE) of the intercept and slope (A_{Total}).

Sample series	Linear relationship	R^2	SE intercept	SE A_{Total}	DOC range (mg L^{-1})	Peak A, A_{Total} range	*n*
Gäddtjärn	DOC = 18.7 (A_{Total}) + 0.23	0.99***	0.04***	0.14***	0.3 to 15.6	0.027 to 0.829	20
Färgeån	DOC = 15.7(A_{Total}) + 0.48	0.99***	0.09***	0.12***	0.2 to 24.0	0.037 to 1.505	20
Öreälven	DOC = 19.9(A_{Total}) – 0.02	0.99***	ns	0.51***	0.2 to 83.6	0.024 to 3.796	17
Nordic Reservoir	DOC = 20.8(A_{Total}) + 0.27	0.99***	0.13*	0.10***	0.1 to 69.9	0.013 to 3.272	42
Swedish Lake Survey	DOC = 20.1(A_{Total}) + 3.2	0.76***	0.28***	0.41***	< 1 to 46.6	< 0.003 to 2.3	554

Significance indicated for *P* values *<0.05, **<0.01, and ***<0.001 and not significant indicated as ns (data are plotted in the Web Appendix, Supplemental Fig. 5).

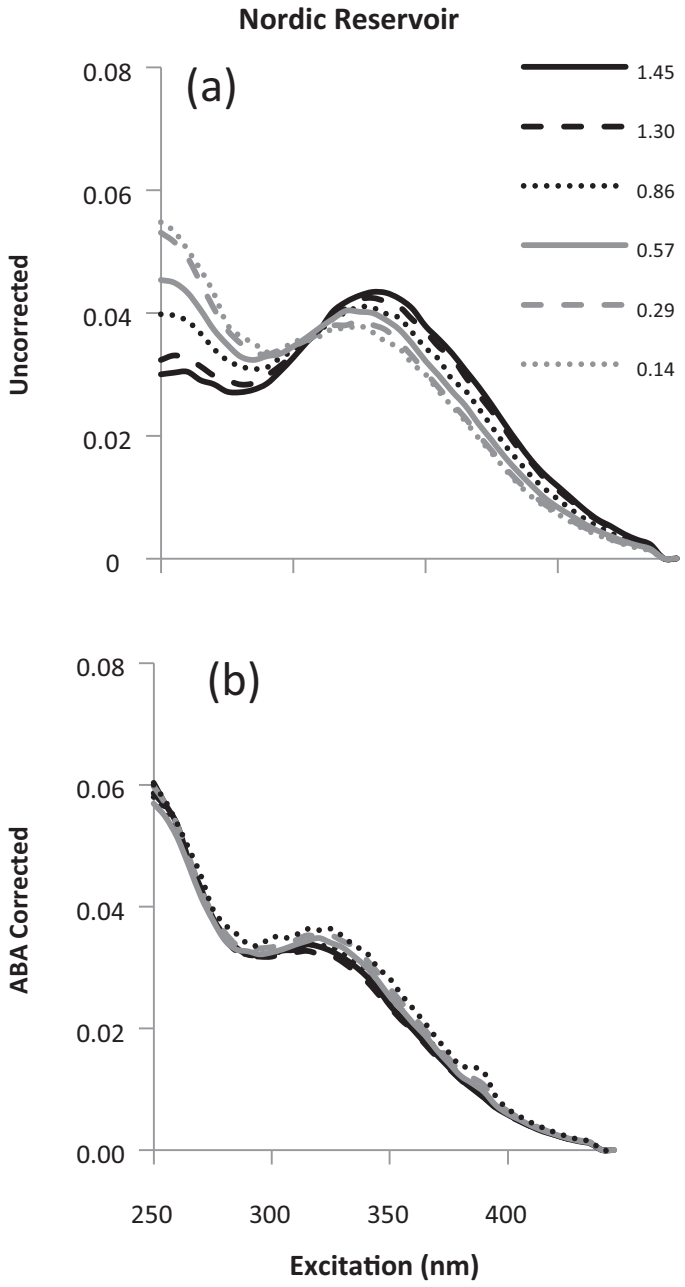

Fig. 2. An example of changes to the shape and positioning of fluorescence Peaks (A and C here) across an excitation spectrum (at λ_{em} 448 nm) of select samples in the Nordic dilution series. Each spectrum was normalized to the integral of fluorescence (λ_{ex} 250 to 445 nm) and scaled by the dilution factor so spectra should be aligned in the absence of inner filter effects. Samples in the dilution series are identified in the legend by the sum of excitation and emission absorbance. The spectra are a) uncorrected, and b) corrected for inner filter effects with ABA.

these two wavelengths ($A_{\lambda ex}$ + $A_{\lambda em}$) is directly related to the suppression of fluorescence intensity due to IFE, and is variable across the EEM, being greatest at shorter excitation and emission wavelengths (Fig. 1c). Thus, the A_{Total} is a more meaningful characterization of absorbance than one arbitrarily chosen wavelength (e.g., A_{254}). In addition, the use of absorbance (also A_{Total}) is in keeping with fundamental literature on fluorescence and IFE (Lakowicz 2006; Miller 1981). For the dilution series, $\lambda_{ex}/\lambda_{em}$ peak maxima for Peaks A, C, and T, were 250/452, 400/520, and 300/352, respectively.

Absorbance-based approach (ABA) for IFE correction

The absorbance-based approach (ABA) (Eq. 2) (Lakowicz 2006) uses the measured absorbance (A_λ) at each pair of excitation (λ_{ex}) and emission wavelengths (λ_{em}) across the EEM to convert the observed fluorescence intensity (F^{obs}) into the corrected fluorescence intensity (F^{corr}). As explained above, the sum of $A_{\lambda ex}$ and $A_{\lambda em}$ at any point on the EEM is the A_{Total}. For example, for Peak T, $A_{Total} = A_{300} + A_{352}$. Since we measured fluorescence in a 1 cm cuvette, and it is assumed that absorbance (excitation) and fluorescence (emission) occurs at the midpoint of the cuvette, the $A_{\lambda ex}$ and $A_{\lambda em}$ were multiplied by 0.5. Model Eq. 2 is described elsewhere in full detail with assumptions (Macdonald et al. 1997).

$$F^{corr}_{\lambda ex,\lambda em} = F^{obs}_{\lambda ex,\lambda em} \times 10^{(0.5\times(A_{\lambda ex}+A_{\lambda em}))} \quad (2)$$

The controlled dilution approach (CDA) for IFE correction

The CDA (Luciani et al. 2009) calculates the inner filter correction from two fluorescence EEMs: the undiluted sample, and a known dilution thereof. The original EEM is modeled as the product of a linear component corresponding to the corrected fluorescence EEM, and a nonlinear component (originally derived in Luciani et al. (2009), Eq. 21). The CDA (Eq. 3) requires the original EEM (F^{obs}), the diluted EEM (pF^{obs}), and the value of the dilution factor (p). Although the sensitivity of the approach is favored by higher dilutions, Luciani et al. (2009) recommend a dilution factor of around two to ensure accurate estimation of the $F^{Corr,CDA}$ while minimizing experimental uncertainty and the loss of signal/noise due to dilution. Luciani et al. (2009) used dilution factors ranging from 2.07 to 2.11 to test the approach.

$$F^{Corr,CDA}_{\lambda_{ex},\lambda_{em}} = \left(\frac{\left(pF^{Obs}_{\lambda_{ex},\lambda_{em}}\right)^p}{F^{Obs}_{\lambda_{ex},\lambda_{em}}} \right)^{\frac{1}{p-1}} \quad (3)$$

Assessing the effectiveness of IFE corrections

The four sample dilution series (Gäddtjärn, Färgeån, Öreälven River, and Nordic Reservoir) were corrected using ACA or CDA, resulting in eight datasets consisting of full EEMs (40 excitation wavelengths × 76 emission wavelengths). Within each EEM dataset, dilution series at each wavelength pair resulted from pairing a vector of fluorescence intensities, and a vector of absorbance values (A_{Total} at the corresponding wavelength pair). Even after regions affected by scattered light are excluded, dilution series at more than 1000 wavelength pairs spanning the EEM remain.

To assess both correction approaches, we tested the linearity between absorbance, A, and fluorescence, F, using robust

linear regressions described below. In the absence of IFE, there is a linear relationship between F and A, as derived from Beer's law (Holland et al. 1977; Miller 1981). This is shown in Eq. 4, where the slope is *m*, and the y-axis intercept is *b*.

$$F = mA + b \quad (4)$$

The slope of the linear regression depends on structural characteristics of the fluorophore including its quantum yield, thus *m* will vary between wavelengths and data sets (sampling sites). The intercept, *b,* should be equal to zero after accounting for background fluorescence/absorbance via blank-subtraction. In the absence of factors contributing to nonlinearity, a perfectly linear relationship between *F* and *A* in Eq. 4 would be reflected in a slope of 1.0 for a relationship between log(*F*) and log(*A*) for all dilution series. Taking the logarithm of both sides of Eq. 4 gives

$$\log(F) = \log(mA + b) = \log(m) + \log(A + b/m) \quad (5)$$

when *b* is exactly zero, and there is no background fluorescence signal, then this simplifies to

$$\log(F) = \log(M) + \log(A) \quad (6)$$

when the relationship between *F* and *A* is truly linear in Eq. 4, a plot of log(*F*) versus log(*A*) will have a slope equal to 1.0 as in Eq. 6. However, slopes in log-log plots that are significantly different from 1.0 can arise from two main sources. First, if the relationship between *F* and *A* is nonlinear, log(*F*) versus log(*A*) may appear linear but with a slope ≠ 1.0. Thus, if *F* trends downwards with increasing *A* (concave down, indicating under-correction) the slope is < 1.0, whereas if *F* trends upwards with increasing *A* (concave up, over-correction) the slope is > 1.0. Second, over-subtracted or under-subtracted background fluorescence causes a non-zero intercept in Eq. 4 and $b/m \neq 0$ in Eq. 5, leading to slopes above or below 1.0, respectively, when log(F) is plotted against log(A).

Theoretically, it has been shown that blank subtraction of fluorescence and absorbance data should remove *b* in Eq.4 and simplify Eq.5 to Eq.6, describing a straight line with a slope of exactly 1.0. In practice, however, it can be difficult to acquire accurate blanks in parts of scans where S/N is low due to instrument limitations and/or susceptibility to trace contamination. This can lead to a significant intercept in Eq. 4 and cause the slope of log(*F*) against log(*A*) to deviate from 1.0. It is important to take these considerations into account when evaluating the linearity of dilution series across a full EEM.

Equations 4-6 show that there is only one relationship between absorbance and fluorescence at any wavelength pair in a sample. In this study, since the equations derived from the ABA and CDA corrected dilution series were not identical, a process for determining the most accurate relationship was required. Since the CDA-corrected dilution series nearly always had much greater variance than ABA-corrected dilution series, F-tests for differences in slope could not be implemented meaningfully. Therefore, since there was no evidence of nonlinearity in the untransformed datasets as long as absorbance remained below 1.5 (e.g., Web Appendix, Supplemental Fig. 3), the equation with slope nearest to 1.0 with a high R^2 (>0.95) was used as the most correct reference relationship.

Regression coefficients were estimated by robust linear regression for log-transformed (Eq. 6) dilution series in each data set with iteratively reweighted least squares fitting and a bi-square weighting function performed in MATLAB (R2012a). Robust linear regression differs from ordinary linear regression in that data points that deviate most from linearity receive lower weightings in the regression, making the fit more 'robust' to the presence of random outliers (Holland and Welsch 1977). An R^2 for the robust fit can be estimated from the ratio of the sum of squares explained by the regression model (SST – SSE) and the total sum of squares (SST) around the mean. We investigated the effectiveness of ABA and CDA across the full EEM, as well as for humic-like Peaks A ($\lambda_{250}/\lambda_{452}$) and C ($\lambda_{350}/\lambda_{452}$), and the protein-like Peak T ($\lambda_{300}/\lambda_{352}$).

Robust regressions were performed separately on each ABA- and CDA-corrected dilution series. All data points with absorbance exceeding 1.5 were excluded, since visual examination indicated these were systematically biased in a positive (ABA) or negative (CDA) direction (see Öreälven and Nordic Peak A as examples, Fig. 4c and d). Similarly, fluorescence intensities with low S/N (Peak T) were positively biased (Fig. 5) and would have skewed the regressions if not removed. The LOR at each wavelength pair was used to identify the absorbance corresponding to the lower limit of accurately reportable fluorescence, and only fluorescence intensities that were above LOR and below $A_{Total} = 1.5$ were included in the regressions. This approach increased the accuracy of linear fitting in EEM regions with low S/N, as was evident for Peak T (Fig. 5a).

Sensitivity of IFE corrections to instrument and experimental error

To better understand the reasons for underlying differences between the two correction methods, a modeling study was implemented by applying ABA and CDA corrections to model an ideal dilution series subject to known levels of error and noise. First, a theoretical EEM was assumed from an average CDA- and ABA-corrected EEM and a theoretical absorbance spectrum assumed equal to the measured spectrum. A 26-sample theoretical dilution series was then constructed, and theoretical inner filter effects were applied to each fluorescence sample using the theoretical absorbance and Eq. 1. Dilutions were evenly spaced along a binary logarithm (base 2) scale, so that all but the most dilute samples could be paired with an exact 2-fold dilution when implementing CDA. A range of scenarios were then tested, by superimposing different levels of background fluorescence (blank), measurement error and random noise on the theoretical EEMs. MATLAB programs to

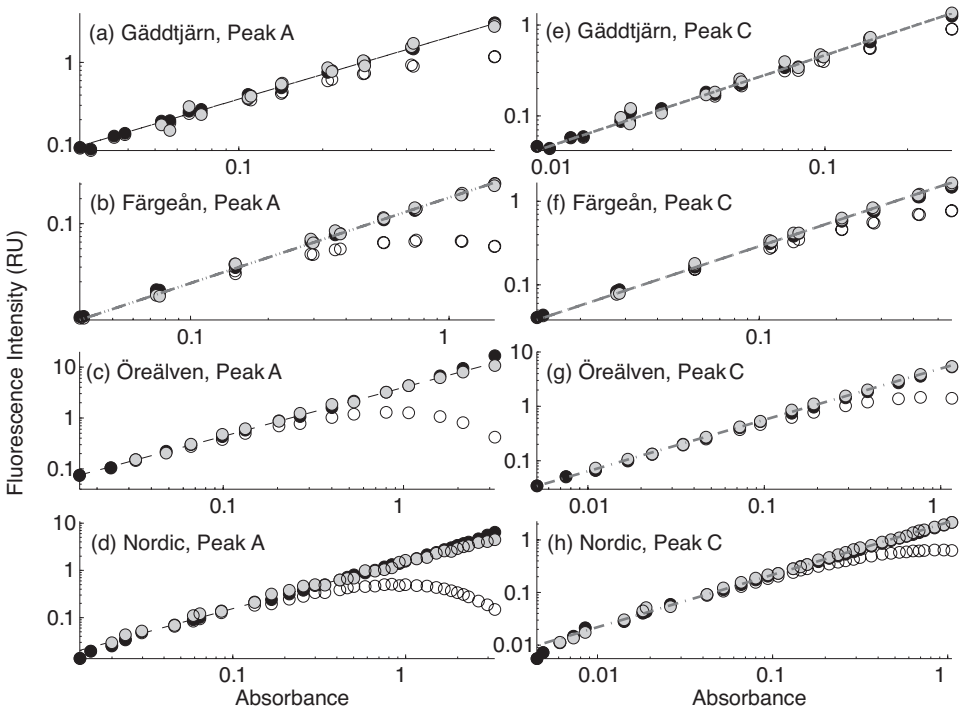

Fig. 3. Relationships between fluorescence intensity in Raman units (R.U.) and absorbance (A_{Total}) at corresponding wavelengths ($\lambda_{ex}/\lambda_{em}$) for Peak A (250/452) and Peak C (350/452) for excitation-emission matrixes that are uncorrected for inner-filter effects (open circles), and those corrected for inner filter effects with ABA (black circles) and CDA (gray circles).

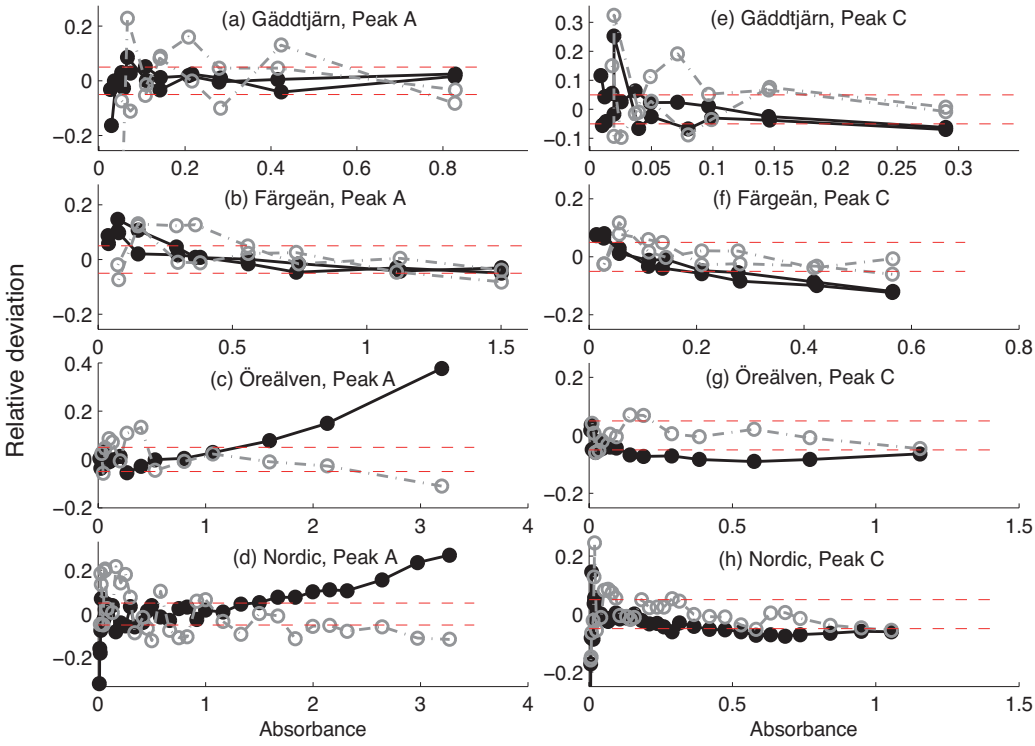

Fig. 4. Plots of relative deviation from the best fit using two approaches to correct for inner filter effects, the ABA, and the CDA, using four samples, Gäddtjärn, Färgeån, Öreälven, and Nordic, relative to the absorbance (A_{Total}) at corresponding wavelengths ($\lambda_{ex}/\lambda_{em}$) for Peak A (250/452) and Peak C (350/452). Horizontal dashes indicate +/- 5% deviation from the linear dilution curve.

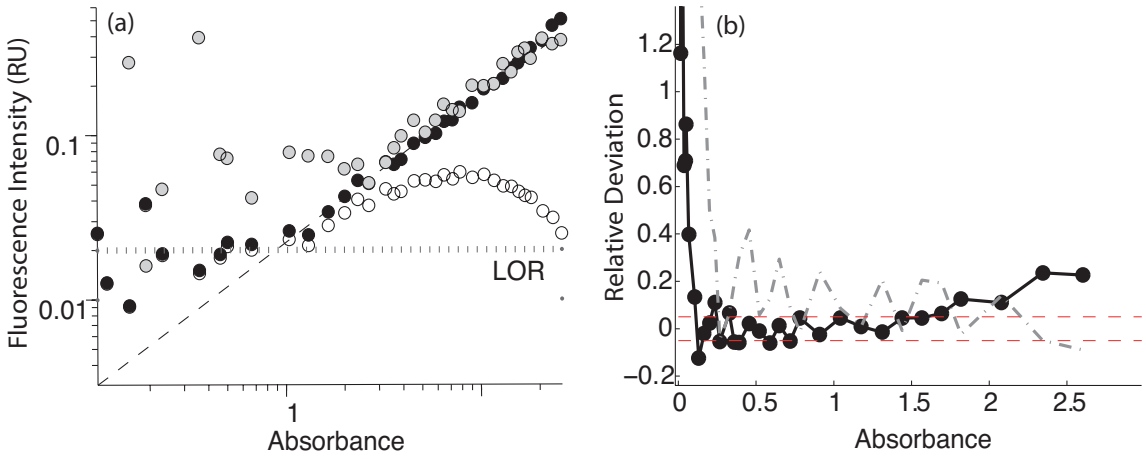

Fig. 5. (a) Relationship between fluorescence intensity in Raman units (R.U.) and absorbance (A_{Total}) at wavelengths ($\lambda_{ex}/\lambda_{em}$) relevant for Peak T (300/352) for Nordic samples uncorrected for inner filter effects (open circles), and after correction using ABA (black circles) and CDA (gray circles). (b) The relative deviation from the line of best fit for corrected data using ABA (black circles) and CDA (open circles).

implement the ABA and CDA algorithms used in this study, together with a program allowing the user to investigate any wavelength pair in the Nordic dataset while assuming levels of experimental error and noise relevant to their own instrumentation and experimental techniques is freely available for download via the drEEM toolbox for MATLAB (Murphy et al. 2013; available at http://models.life.ku.dk/drEEM).

Exploring the use of ABA across a Lake Survey

The effectiveness of ABA correction was further explored using Lake Survey samples with $A_{Total} < 1.5$. For illustrative purposes, our analyses focuses on two commonly known fluorescence peaks experiencing the greatest IFE, i.e., Peaks A and T. Fluorescence and absorbance were linearly related to Peak A, but not for Peak T. Thus, nonlinearity in the Peak T relationship was further explored in relation to chemical variables (nitrate, calcium, pH, metals, etc.) in a stepwise manner.

Assessment

Comparison of fluorescence spectra with and without IFE

The suppression of fluorescence due to IFE was apparent in all uncorrected datasets, most obviously for highly concentrated samples. Changes to the shape and intensity of uncorrected fluorescence spectra due to IFE are evident from Fig. 2, which shows the uncorrected (Fig. 2a) and ABA-corrected (Fig. 2b) excitation spectra at λ_{ex} 448 (passing through Peaks A and C) of samples in the Nordic dilution series. Spectral distortions due to IFE are seen to be greatest at shortest wavelengths where absorbance is highest (Fig. 1c). IFE correction using the ABA clearly realigned the spectra in terms of both intensity and shape (Fig. 2b).

Assessing the effectiveness of ABA and CDA

Deviations from the theoretical 1.0 slope of the log-log F versus A curve were evaluated to assess the effectiveness of the ABA and CDA correction approaches for Peak A, C (Fig. 3 and 4), and T (Fig. 5). In the Peak A region, slopes of ABA- and CDA-corrected datasets were near 1.0 for all four data sets (Table 2). In the Peak C region, CDA slopes were generally close to 1.0, whereas ABA slopes were slightly lower in the Färgeån, Öreälven, and Nordic datasets (Table 2). In the Peak T region, slopes of both ABA- and CDA-corrected datasets were lower than in other regions of the EEM, with CDA slopes lower than ABA slopes (Table 2). In general, for the three Peaks of interest, the slope of log-log regressions ranged from 0.90 to 1.05 with the ABA approach, and from 0.51 to 1.05 with the CDA approach (Table 2). Deviations from the line of best fit (i.e., the regression line with slope nearest 1.0) are illustrated in Fig. 4 and 5b. Larger deviations occurred consistently at low A_{Total}, where experimental error was largest and S/N lowest (Fig. 4 and 5b). When the log-log regression was extended beyond an absorbance of 1.5 for Öreälven and Nordic (Fig. 4c and d), the ABA and CDA dilution series diverged with ABA consistently over-correcting and CDA consistently under-correcting these most concentrated samples. Thus, an A_{Total} of 1.5 was considered the upper limit for effective corrections using both CDA and ABA. The slope for regressions were assessed across all wavelength pairs, where it became evident that ABA corrected datasets had R^2 lying between 0.90 and 1.05 whereas CDA-corrected datasets contained some regions with slope < 0.90 (Fig. 6). Regressions near the Peak T region where many data points were below the LOR were omitted (Fig. 6).

Apparent under-correction of Peak C using ABA was observed in other regions of the EEM with longer λ_{ex} (>350 nm) (e.g., Nordic, Fig. 6d). This under-correction could be traced back to underestimated absorbance at $A_{\lambda} > 350$ nm resulting in underestimated IFE correction factors using the ABA method. There are two main reasons why absorbance can be under-estimated during measurement: i) stray light in the instrument, which is most severe when absorbance is highest

Table 2. Coefficients (slope *M*, intercept *B*) in robust linear regressions between the natural logarithm of total absorbance (A_{Total}) at specific wavelengths (λ_{ex} λ_{em}) corresponding to Peaks A, C, and T, and the logarithm of fluorescence intensity, i.e., log $F = M \log A_{Total} + B$, for four water sources corrected for inner filter effects using ABA or CDA. The slope (*m*) of the untransformed dataset was calculated from $m = e^B$. Also shown are the coefficient of determination (R^2), degrees of freedom (*df*), and the probability (*p*) that the *m* equaled 1.0.

Sample	Method	Peak	λ_{ex}	λ_{em}	*M* ±	SE	*B* ±	SE	*m*	R^2	*df*	*p*
Gäddtjarn	ABA	A	250	452	1.00	0.02	1.28	0.04	3.60	1.00	8	0.80
	CDA	A	250	452	0.99	0.08	1.25	0.14	3.50	0.98	6	0.86
	ABA	C	350	452	1.00	0.02	1.48	0.05	4.38	1.00	8	0.80
	CDA	C	350	452	1.00	0.05	1.54	0.14	4.65	0.99	6	0.99
	ABA	T	300	352	0.98	0.04	–1.03	0.08	0.36	0.99	5	0.60
	CDA	T	300	352	1.05	0.24	–0.88	0.45	0.41	0.93	5	0.85
Färgeån	ABA	A	250	452	1.00	0.01	0.69	0.01	1.99	1.00	6	0.78
	CDA	A	250	452	1.03	0.03	0.72	0.05	2.06	1.00	5	0.43
	ABA	C	350	452	0.96	0.01	0.96	0.01	2.62	1.00	7	0.00
	CDA	C	350	452	1.01	0.02	1.10	0.03	2.99	1.00	6	0.39
	ABA	T	380	480	0.96	0.01	1.05	0.02	2.85	1.00	7	0.00
	CDA	T	380	480	1.02	0.02	1.23	0.05	3.42	1.00	6	0.34
Öreälven	ABA	A	250	452	0.96	0.01	1.38	0.01	3.98	1.00	11	0.00
	CDA	A	250	452	0.96	0.02	1.41	0.04	4.10	1.00	9	0.06
	ABA	C	350	452	0.93	0.00	1.51	0.01	4.53	1.00	14	0.00
	CDA	C	350	452	0.94	0.01	1.60	0.02	4.97	1.00	12	0.00
	ABA	T	300	352	1.05	0.08	–1.22	0.11	0.29	1.00	7	0.54
	CDA	T	300	352	1.01	0.30	–1.17	0.43	0.31	0.66	7	0.97
Nordic	ABA	A	250	452	1.00	0.01	0.43	0.01	1.54	1.00	20	0.83
	CDA	A	250	452	0.95	0.02	0.39	0.03	1.48	0.99	20	0.01
	ABA	C	350	452	0.97	0.00	0.69	0.01	1.99	1.00	33	0.00
	CDA	C	350	452	1.00	0.01	0.77	0.02	2.15	1.00	31	0.60
	ABA	T	300	352	0.90	0.02	–1.75	0.03	0.17	0.99	20	0.00
	CDA	T	300	352	0.51	0.06	–1.76	0.08	0.17	0.79	20	0.00

and does not explain underestimated absorbance at longer wavelengths, or ii) interfering light due to sample fluorescence during absorbance measurements (Upstone 2000). The latter is likely the contributing factor here. When samples fluoresce during absorbance measurement, there are two phenomena contributing to the measurement of transmitted light energy rather than one, which can result in an underestimation of sample absorbance (Upstone 2000). This could explain the observed under-correction by ABA in the Peak C region, where absorbance is typically low, yet fluorescence is relatively high.

Fluorescence intensities in the Peak T region were not apparent for data sets except Nordic, resulting in slopes that were often significantly different from 1.0 (Table 2). In the case of the Nordic datasets, ABA resulted in a better correction of Peak T than did CDA (Table 2, Fig. 5). Similar to the results for Peak A, the ABA effectively corrected Peak T up to an A_{Total} of around 1.5 despite fluorescence intensities that were an order of magnitude lower (Fig. 5a), demonstrating that the upper absorbance limit to IFE correction is indeed independent of wavelength pair. In the low A_{Total} range (<0.04) of Peak T, ABA-corrected fluorescence intensities were very similar to uncorrected fluorescence intensities, as would be expected due to low (<5%) IFE effects (Fig. 5a). Thus, the error when A_{Total} was < 0.04 is rather due to extremely low fluorescence intensity (nearing the instrument LOR), rather than the correction approach. The relatively low slope (0.90) associated with ABA-corrected Peak T can be explained by incomplete blank subtraction and interferences from dark current, as seen by the positive y-intercept in the untransformed dilution series (Web Appendix, Supplemental Fig. 3c), i.e., $b/m > 0$ in Eq. 5. Overall, slopes significantly less than 1.0 in the protein like regions of the EEM (Fig. 6) can be attributed to the presence of residual fluorescence. Residual fluorescence has a greater impact on the slope of Peak T compared with Peak A or C due to the far lower overall intensity. The low slope (0.74) and poorer fit (R^2 = 0.91) of CDA-corrected Peak T (Table 2, Fig. 5b) is the result of over-estimated CDA-corrected fluorescence when S/N was low (Fig. 5b). Results for Peak T in the Nordic dilution series clearly demonstrated that ABA more effectively corrected fluorescence than did CDA in the presence of residual fluorescence when S/N is low (Fig. 5).

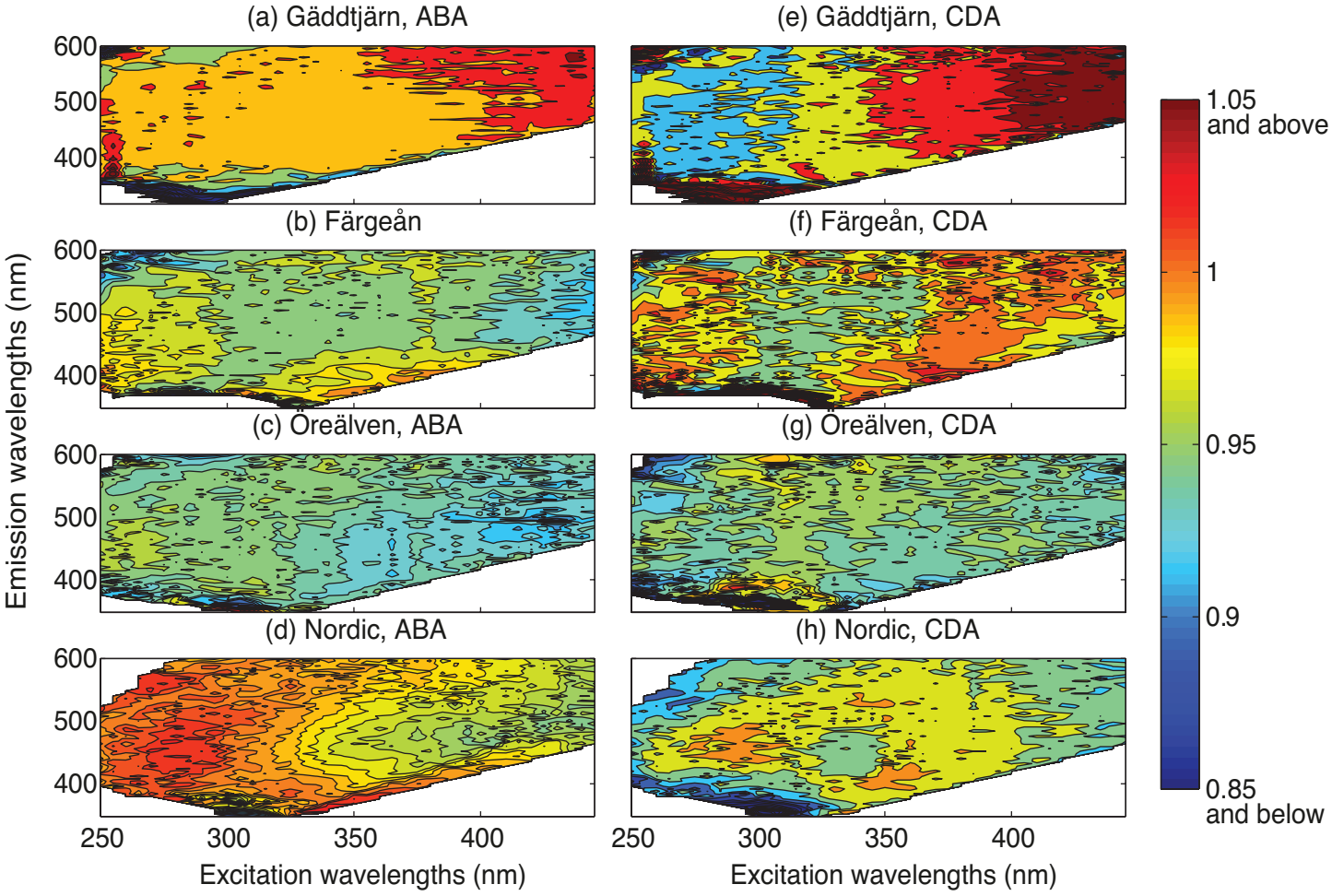

Fig. 6. EEM showing slopes of log-log relationships between fluorescence and absorbance for dilution series of four samples (Gäddtjärn, Färgeån, Öreälven, and Nordic) corrected using ABA or CDA. EEM regions with too few data above reporting limits have missing slopes.

Modeling the interaction between measurement error and IFE correction

The modeling study used samples from the Nordic dataset to generate a theoretical EEM, its absorbance spectrum, and a Milli-Q blank. Random noise and instrument bias were superimposed on the theoretical samples to investigate the effects of measurement error on ABA- and CDA-corrected fluorescence intensities. Seven cases were developed to represent the influence of background signals, random noise, and instrument bias on absorbance and fluorescence measurements, and combinations thereof. Assumed amplitudes of random noise were equal to measured values for the instruments in this study (fluorometer: 5×10^{-4} R.U., spectrophotometer 1×10^{-3}). As mentioned above, an apparent under-correction of Peak C was noticed when using ABA (at $\lambda_{ex} > 350$ nm), which may have been due to a negative bias in absorbance spectra. Accordingly, a 3% negative bias in the absorbance spectra was assumed to affect wavelengths above 325 nm, to simulate humic fluorescence interference in the absorbance measurement. The error in dilution factors was assumed as ± 1%, which was similar to error associated with gravimetric dilution in this study, although they may be lower than for volumetric dilution. The results of this modeling study are demonstrated for Peak A in Fig. 7. When it was assumed that fluorescence and absorbance measurements were completely accurate and incorporated no noise or unsubtracted background fluorescence, both approaches accurately reproduced the ideal dilution series (Case 1). When random bi-directional noise was introduced to the fluorescence spectra (Case 2), the variability in the CDA dilution series was of greater amplitude than in the ABA dilution series, although the scale of error was very small. In Case 3, 1% noise plus 3% bias in the absorbance spectra were propogated to ABA whereas 1% error in the dilution factor (Case 4) was propagated to CDA. The observed high sensitivity of CDA to small dilution errors is the basis of the CDA developers' recommendation to select a dilution factor that minimizes experimental uncertainty (Luciani et al. 2009). Both methods were sensitive to background fluores-

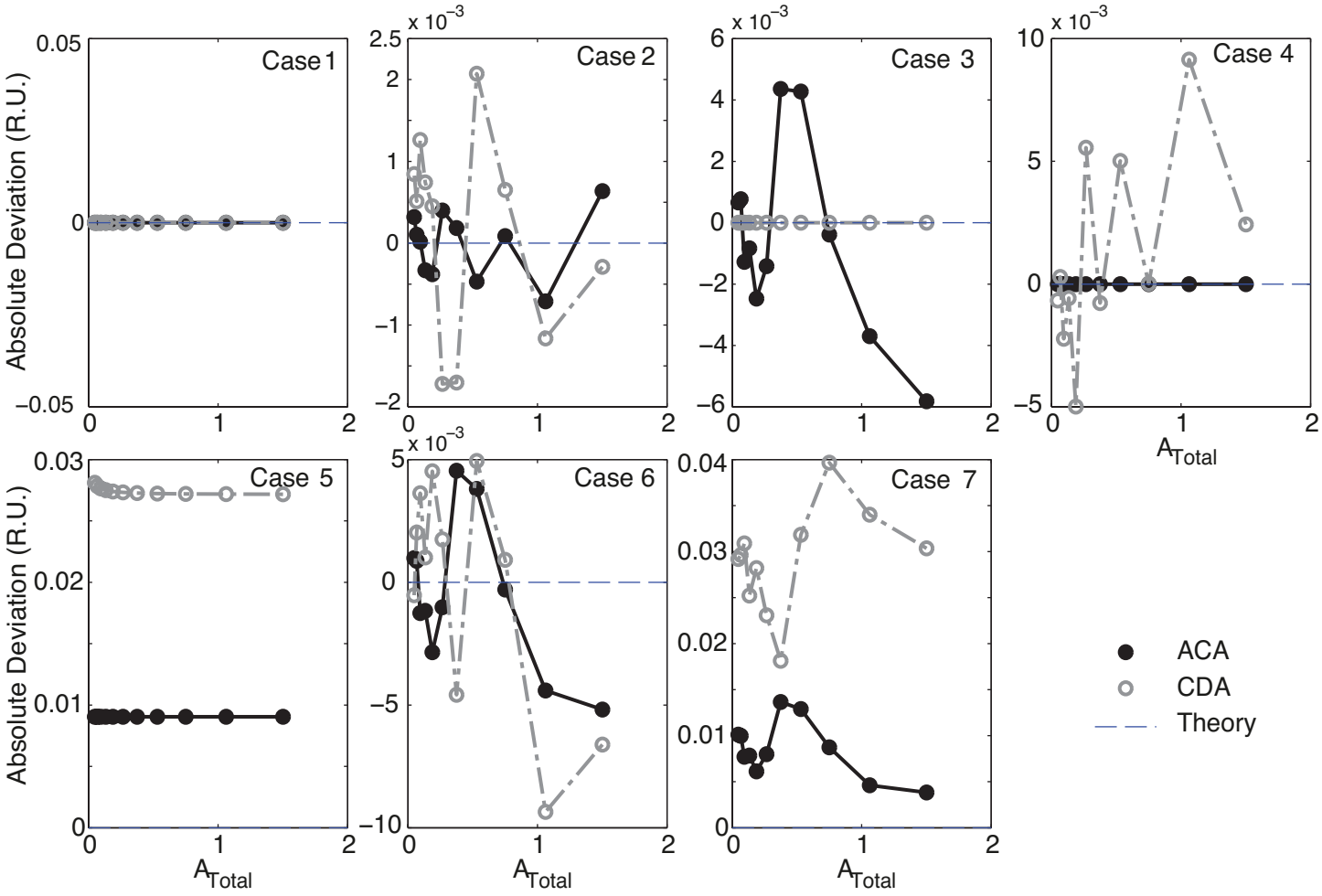

Fig. 7. Demonstration of the effects of measurement error on the accurancy of IFE using a modeling approach. Results are demonstrated for dilution series of Nordic Peak A using the ABA (black dots) and CDA (open circles). Plots depict deviation from a theoretical dilution series under seven scenarios: Case (1) no error or noise, Case (2) random EEM noise, Case (3) absorbance spectrophotometer noise and bias, case (4) 1% dilution error, case (5) unsubtracted EEM blank, case (6) all noise/error except unsubtracted EEM blank, case (7) all random noise/error plus unsubtracted EEM blank. Note the variable scale on the Y-axis.

cence signals (unsubtracted blank, Case 5), which resulted in over-correction of fluorescence, particularly at low signal/noise and lower regression slopes, and affected CDA to a greater extent than ABA. Case 6 shows the combination of cases excluding the unsubtracted blank EEM, whereas Case 7 shows the combination of all errors and biases. Under the assumptions of this model, the dilution factor error and background fluorescence (unsubtracted blank) were the most important factors contributing to inaccuracy of inner filter corrections. Overall, the ABA approach appeared to be most robust to instrument noise and biases.

The modeling study is valid only within the linear range where Eq. 1 applies. At higher absorbances (approx. $A_{Total} > 1.5$ in this study), differences between the geometrical parameters of the fluorescence spectrophotometer excitation and emission beams versus the theoretical instrument biases described by the equation lead to the overestimation of IFE, with the result that ABA begins to overcorrect fluorescence if individual instrument parameters are not taken into account (Christmann et al. 1980; Gu and Kenny 2009; Holland et al. 1977). Further details explaining the overestimation of IFE is explained in the Web Appendix.

Exploration of ABA with a nationwide lake survey

To explore the effect of ABA correction across natural lake water samples, we examined uncorrected and corrected fluorescence intensities for Peaks A and T across the Lake Survey (Fig. 8). The $\lambda_{ex}/\lambda_{em}$ pair for Peaks A (250/448) and T (270/368) were identified as the point on EEMs (n = 562) with most frequent maximum intensity across areas typically associated with these peaks (Coble et al. 1990; Fellman et al. 2010), thus Peak T wavelength location differs slightly from samples in the dilution series. We examined simple linear regressions of both the log-log transformed datasets (Eq. 5) as well as untransformed datasets (Eq. 4). Uncorrected fluorescence

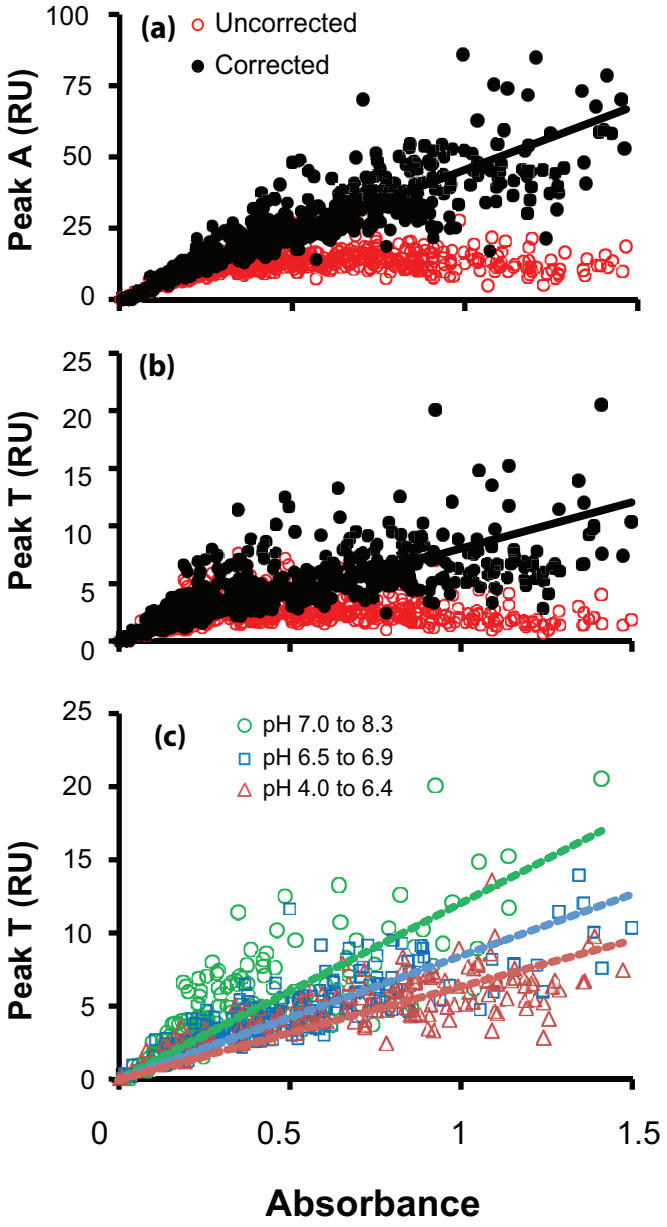

Fig. 8. Fluorescence intensity for (a) Peak A ($\lambda_{ex}/\lambda_{em}$ = 250/448) and (b) Peak T ($\lambda_{ex}/\lambda_{em}$ = 270/368) in a nationwide Lake Survey. Spectra are uncorrected (open circles) and corrected (black circles) for inner filter effects using ABA, in relation to the sum of absorbance (A_{Total}) at excitation-emission wavelengths ($\lambda_{ex}/\lambda_{em}$) corresponding to the Peak. (c) The relationship between corrected Peak T fluorescence and A_{Total} when samples were subdivided into three pH groups: pH 4.0 to 6.4 (open triangles), 6.5 to 6.9 (open circles), and 7.0 to 8.3 (open squares). Only data with A_{Total} < 1.5 are included.

intensities for Peaks A and T were increasingly suppressed with increasing absorbance (Fig. 8a and b). After correction for IFE using ABA, the log-log regression of Peak A fluorescence against absorbance was nearly linear with a slope near 1.0 (log-log slope = 0.96, R^2 = 0.89, Table 3), despite the wide range of lake water samples included in the dataset with varying DOM and ionic composition. For Peak T, the ABA correction improved the linearity of the relationship between fluorescence and absorbance relative to uncorrected data (Fig. 8b), yet the slope of the log-log relationship was far lower (M = 0.76), as was the coefficient of determination (R^2 = 0.72, Table 3, shown in Web Appendix Supplemental Fig. 4). However, after subdividing Lake Survey samples into three pH groups of approximately equal size, it was clear that the slope was influenced by pH, with the most acidic sites having the greatest suppression of fluorescence, despite effective correction of IFE (Fig. 8c, Table 3). The quenching effects by H^+ apparent for Peak T were far less apparent for Peak A across the widely distributed pH values in this dataset (4.0 to 8.3). The weakest relationship (R^2 = 0.72) was observed in the lowest pH group (4.0 to 6.4), although it could be improved with further subdivision (not shown).

Discussion

This is the first study to attempt a comprehensive evaluation of simple IFE correction approaches on DOM fluorescence spectra across full EEM. Quantifying the influence of IFE on DOM fluorescence spectra is nontrivial, requiring consideration of several factors, including experimental error such as dilution errors, variations in instrument sensitivity, and accuracy across the EEM, including signal-to-noise ratios, as well as attention to factors other than IFE influencing non-linearity, including quenching. We assessed linearity across full EEMs in dilution series of samples from four sites spanning a range of absorbance relevant to surface waters. Both the ABA and CDA correction resulted in adequate correction of the EEMs, including Peaks A, C, and T up to an absorbance of at least 1.5. The protein-like Peak T region was also linear up to an absorbance of 1.5, however, the combination of high IFE, lower signal-to-noise, and sporadic contamination can more readily affect the Peak T region than Peaks A and C, especially in CDA-corrected datasets. Clearly, studies adopting the criterion of A_{254} = 0.3 to be the upper threshold for effective algebraic correction have grossly underestimated their applicability.

When do IFE commence?

A universal threshold absorbance indicating the point when IFE emerge as significant can be calculated directly from Eq. 1(Miller 1981). For instance, the value of absorbance corresponding to when IFE suppress fluorescence by 1% at any point on the EEM is calculated as log (0.01)/0.5 = 0.0086 in a 1 cm cuvette. Likewise, a suppression of fluorescence by 5% due to IFE equates to an absorbance of 0.042. Based on this same approach, Lakowicz (2006) suggests that absorbance should be less than 0.05 to avoid inner filter effects, corresponding to a 6% suppression of fluorescence. Absorbance thresholds reported by other studies (for example, Lakowicz 2006; Miller 1981) do not give reference to a specific wavelength, likewise we too present an upper limit that is not restricted to one wavelength but rather universal to all excitation-emission wavelength pairs (A_{Total}). Of the 554 Swedish lakes used in this study,

Table 3. Variables derived from relationships between fluorescence intensity (F) of Peaks A and T, along with Peak T sub-divided into three pH groups, and absorbance (A,: $A_{Total} = A_{\lambda ex} + A_{\lambda em}$ for Peak of interest) for Lake Survey samples collected across Sweden (n = 554), including the slope (m) and intercept (b) of the linear relationship, and the slope (M) and intercept (B) of the of the log-log transformed relationship. All relationships were statistically significant at $P < 0.0001$.

Fluorescence Peak	λ_{ex} / λ_{em}	*m*	*b*	*Linear R²*	*M*	*B*	log-log R²	*n*
Peak A	250/448	39.9	4.4	0.71	0.96	3.8	0.89	554
Peak T	270/368	5.48	1.87	0.27	0.76	2.05	0.72	554
Peak T: pH 4.0 to 6.4	270/368	4.37	1.76	0.56	0.68	1.83	0.81	161
Peak T: pH > 6.4 to < 7.0	270/368	6.66	1.20	0.68	0.78	2.05	0.82	186
Peak T: pH 7.0 to 8.3	270/368	10.15	1.00	0.61	1.01	2.55	0.72	207

only 20 lakes (3%) had an $A_{Total} < 0.05$ and thus the vast majority of lake water samples required IFE correction. Lakes for which EEMs did not require correction had DOC ≤ 2.1 mg C L^{-1}. For further comparison, in a compilation of DOC concentrations from 7514 lakes distributed over six continents, a median DOC concentration of 5.7 mg C L^{-1} was reported (Sobek et al. 2007). This demonstrates the general necessity to correct for IFE in the vast majority of lake water samples.

Can sample dilution effectively remove IFE?

In contrast to open ocean waters, most surface water samples from inland waters as well as estuaries likely impart some IFE, even if the sample appears to be optically clear. The fact that IFE are significant even when absorbance is relatively low indicates that in many cases, IFE correction may be necessary despite applying substantial dilution factors. For instance, Gäddtjärn and Färgeån have DOC concentrations of 15.6 and 24.0 mg/L, which is common in Fennoscandian lakes, and would require dilution factors as high as 21 and 38 times, respectively, to achieve absorbance below 0.04. Dilution factors of this magnitude are unsafe, considering the risks of dilution error and contamination. In addition, dilution factors high enough to reduce absorbance to < 0.04 will result in very low S/N across much of an EEM. In this study, dilution was most accurate when determined gravimetrically, or from relative absorbance, followed by relative DOC concentrations and last by volumetric methods (pipette and volumetric flask) (Web Appendix, Supplemental Fig. 1). Changes in pH are a consideration when imposing large dilutions. If pH is significantly changed by dilution the configuration of DOM structures, and subsequently, the optical properties may change (Pace et al. 2012; Patel-Sorrentino et al. 2002; Spencer et al. 2007). In our case, pH variability was relatively small across the dilution series since the original pH of samples was close to that of the medium used to dilute samples (Milli-Q water) and likely caused minimal optical change (Spencer et al. 2007). Whereas altered optical properties due to the relatively small shifts in pH are incorporated within these dilution series, any change due to pH did not significantly affect linearity up to an absorbance of 1.5 in this study.

Thus, applying large dilution factors to entirely avoid inner filter effects is inadvisable. Results from this study illustrate that dilution is unnecessary when absorbance is below 1.5, since ABA or CDA correction allows accurate compensation for IFE effects. At higher absorbance (>1.5), a 2-fold dilution followed by ABA or CDA correction would be sufficiently large in the vast majority of cases.

Attributes and limitations of ABA and CDA

One of the key advantages of the ABA is its relative ease of use and effectiveness across a wide range of absorbance, whereas its main disadvantage is the need for an additional absorbance instrument. Obviously, errors in absorbance measurements are transferred to the fluorescence spectra during IFE correction and the upper limit of the absorbance spectrophotometer may be a limiting factor. To avoid variability due to differences in band widths and spectral distributions between light sources, it is preferable to use the same light source for measuring fluorescence as for absorbance (Gilmore et al. 2012; Miller 1981). New spectrofluorometers have recently entered the market with the capacity to measure fluorescence and absorbance simultaneously, allowing for more direct and accurate IFE corrections. However, when ABA is used with separate absorbance and fluorescence spectrophotometers, differences between analyses can be minimized by using the same quartz cuvette in both instruments, and analyzing optical properties as close in time as possible.

A key advantage of CDA is that it does not require instrumentation additional to the fluorescence spectrophotometer. It was also suggested that since the sensitivity of measurement is greater for fluorescence compared with absorbance, CDA is likely to be more accurate than the ABA (Luciani et al. 2009). However, our modeling study indicated that small dilution errors (even 1%) can lead to similar variability in CDA-corrected fluorescence intensity as would larger errors (3%) plus bias in absorbance measurement for ABA. Whereas ABA typically outperformed CDA in the Peak A and T regions, CDA outperformed ABA in the Peak C region. Both methods therefore appear to have a role to play depending on which wavelengths are of greatest interest in any particular study. Also, the sensitivity of available instrumentation and measurement protocols affect the IFE methods differently and are likely to vary between laboratories.

Quenching of protein-like fluorescence by pH

Failure to distinguish between quenching effects and inner filter effects can lead to the misinterpretation of fluorescence

measurements, as discussed in numerous previous studies (Miller 1981; Parker and Rees 1962; Puchalski et al. 1991). In the Lake Survey, quenching by H^+ had a clear influence on the linearity of Peak T (Fig. 8), which showed decreasing fluorescence with decreasing pH as has been reported previously in other regions of the EEM (Mobed et al. 1996; Patel-Sorrentino et al. 2002). Considerable variability was observed in the fluorescence-absorbance relationships across the Lake Survey due to a multitude of compositional differences in DOM and inorganic ions (Baker et al. 2007; Henderson et al. 2009). Studies of pure tryptophan have reported that increasing protonation of the indole group with increasing acidity quenches this key fluorophore group (Sun et al. 2010; White 1959). Since the isoelectric point of pure tryptophan is 5.90, any tryptophan bound as proteins, peptides, or free amino acids in the DOM of acidic lakes (4.0 to 6.4, and particularly those with pH lower than 5.90), would have greater protonation and the greatest amount of quenching. In contrast, lake samples with pH greater than 5.90 (pH groups 6.5 to 6.9, and 7.0 to 8.3, Fig. 8) would have higher fluorescence due to more deprotonation of tryptophan indole groups, with reduced fluorescence quenching. Overall, this suggests that nonlinear relationships observed between Peak T fluorescence intensity and absorbance were largely a function of quenching by H^+ in the most acidic lakes.

Conclusion and recommendation

Inner filter effects are prevalent in the vast majority of lake waters samples, including samples with apparently low absorbance (1% IFE: 0.008, 5% IFE: 0.042). Currently, there is no standardized approach to correct DOM samples for IFE. However, we found that one of the most commonly applied approaches, ABA (Eq. 1), adequately corrected for IFE in DOM samples up to an absorbance of 1.5, which represents the vast majority of boreal lakes. The newer CDA was also successful in the same absorbance range as long as dilution factors were accurately determined, and the signal-to-noise level was sufficiently high. In the rare case of very highly absorbing samples ($A_{Total} > 1.5$), dilution before IFE correction may be warranted. Yet, only a small 2.0 × dilution factor is attractive, because it minimizes various additional sources of error (measurement, contamination, and quenching) and would be sufficient to subsequently correct for inner filter effects using either of the two algebraic approaches (ABA or CDA). We recommend dilution factors be calculated precisely, either gravimetrically or by using the integrated area of the absorbance spectra. In many cases, applying dilution factors large enough to remove inner filter effects entirely would significantly decrease signal to noise and may introduce additional sources of error, and is not recommended. When assessing the effectiveness of correction approaches, it is necessary to be aware of factors other than inner filter effects that can contribute to nonlinearity between fluorescence and absorbance, including quenching and instrument sensitivity.

References

Baker, A., D. Ward, S. H. Lieten, R. Periera, E. C. Simpson, and M. Slater. 2004. Measurement of protein-like fluorescence in river and waste water using a handheld spectrophotometer. Water Res. 38:2934-2938 [doi:10.1016/j.watres.2004.04.023].

———, S. Elliott, and J. R. Lead. 2007. Effects of filtration and pH perturbation on freshwater organic matter fluorescence. Chemosphere 67:2035-2043 [doi:10.1016/j.chemosphere.2006.11.024].

Birdsall, B., and others. 1983. Correction for light-absorption in fluorescence studies of protein-ligand interactions. Anal. Biochem. 132:353-361 [doi:10.1016/0003-2697(83)90020-9].

Braslavsky, S. E. 2007. Glossary of terms used in Photochemistry 3(rd) Edition (IUPAC Recommendations 2006). Pure Appl. Chem. 79:293-465 [doi:10.1351/pac200779030293].

Christmann, D. R., S. R. Crouch, J. F. Holland, and A. Timnick. 1980. Correction of right-angle molecular fluorescence measurements for absorption of fluorescence radiation. Anal. Chem. 52:291-295 [doi:10.1021/ac50052a019].

Coble, P. G. 1996. Characterization of marine and terrestrial DOM in seawater using excitation emission matrix spectroscopy. Mar. Chem. 51:325-346 [doi:10.1016/0304-4203(95)00062-3].

———, S. A. Green, N. V. Blough, and R. B. Gagosian. 1990. Characterization of dissolved organic matter in the black sea by fluorescence spectroscopy. Nature 348:432-435 [doi:10.1038/348432a0].

———, C. A. Schultz, and K. Mopper. 1993. Fluorescence contouring analysis of DOC intercalibration experiment samples—A comparison of techniques. Mar. Chem. 41:173-178 [doi:10.1016/0304-4203(93)90116-6].

Eftink, M. R. 1997. Fluorescence methods for studying equilibrium macromolecule-ligand interactions. Methods Enzymol. 278:221-257 [doi:10.1016/S0076-6879(97)78013-3].

Fellman, J. B., E. Hood, and R. G. M. Spencer. 2010. Fluorescence spectroscopy opens new windows into dissolved organic matter dynamics in freshwater ecosystems: A review. Limnol. Oceanogr. 55:2452-2462 [doi:10.4319/lo.2010.55.6.2452].

Gilmore, A., R. Hurteaus, S. Fitzgerald, and A. Knowles. 2012. Moving towards a technical specification for fluorescence excitation emission mapping and absorbance analysis of colored dissolved organic matter. WIT Trans. Ecol. Environ. 160:295-306 [doi:10.2495/DN120261].

Gu, Q., and J. E. Kenny. 2009. Improvement of inner filter effect correction based on determination of effective geometric parameters using a conventional fluorimeter. Anal. Chem. 81:420-426 [doi:10.1021/ac801676j].

Henderson, R. K., A. Baker, K. R. Murphy, A. Hamblya, R. M. Stuetz, and S. J. Khan. 2009. Fluorescence as a potential

monitoring tool for recycled water systems: A review. Water Res. 43:863-881 [doi:10.1016/j.watres.2008.11.027].

Holland, J. F., R. E. Teets, P. M. Kelly, and A. Timnick. 1977. Correction of right-angle fluorescence measurements for absorption of excitation radiation. Anal. Chem. 49:706-710 [doi:10.1021/ac50014a011].

Holland, P. W., and R. E. Welsch. 1977. Robust regression using iteratively reweighted least-squares. Communications in statistical theory and methods. A6(9):813-827 [doi:10.1080/03610927708827533].

Hudson, N., A. Baker, and D. Reynolds. 2007. Fluorescence analysis of dissolved organic matter in natural, waste and polluted waters—A review. River Res. Applic. 23:631-649 [doi:10.1002/rra.1005].

Kragh, T., M. Sondergaard, and L. Tranvik. 2008. Effect of exposure to sunlight and phosphorus-limitation on bacterial degradation of coloured dissolved organic matter (CDOM) in freshwater. FEMS Microbiol. Ecol. 64:230-239 [doi:10.1111/j.1574-6941.2008.00449.x].

Lakowicz, J. R. 2006. Principles of fluorescence spectroscopy, 3rd ed. Springer-Verlag [doi:10.1007/978-0-387-46312-4].

Larsson, T., M. Wedborg, and D. Turner. 2007. Correction of inner-filter effect in fluorescence excitation-emission matrix spectrometry using Raman scatter. Anal. Chim. Acta 583:357-363 [doi:10.1016/j.aca.2006.09.067].

Lawaetz, A. J., and C. A. Stedmon. 2009. Fluorescence intensity calibration using the Raman scatter peak of water. Appl. Spectrosc. 63:936-940 [doi:10.1366/000370209788964548].

Luciani, X., S. Mounier, R. Redon, and A. Bois. 2009. A simple correction method of inner filter effects affecting FEEM and its application to the PARAFAC decomposition. Chemometrics Intell. Lab. Syst. 96:227-238 [doi:10.1016/j.chemolab.2009.02.008].

Macdonald, B. C., S. J. Lvin, and H. Patterson. 1997. Correction of fluorescence inner filter effects and the partitioning of pyrene to dissolved organic carbon. Anal. Chim. Acta 338:155-162 [doi:10.1016/S0003-2670(96)00306-6].

Miller, J., N. 1981. General considerations on fluorescence spectrometry. *In* J. N. Miller [ed.], Standards in fluorescence spectrometry, Utraviolet Spectrometry Group. Chapman and Hall/Methuen, Inc.

Mobed, J. J., S. L. Hemmingsen, J. L. Autry, and L. B. Mcgown. 1996. Fluorescence characterization of IHSS humic substances: Total luminescence spectra with absorbance correction. Environmental Science & Technology 30:3061-3065 [doi:10.1021/es960132l].

Murphy, K. R., K. D. Butler, R. G. M. Spencer, C. A. Stedmon, J. R. Boehme, and G. R. Aiken. 2010. Measurement of dissolved organic matter fluorescence in aquatic environments: An interlaboratory comparison. Environmental Science & Technology 44:9405-9412 [doi:10.1021/es102362t].

———, C. A. Stedmon, D. Graeber, and R. Bro. 2013. Fluorescence spectroscopy and multi-way techniques. PARAFAC. Anal. Methods 5:6557-6566 [doi:10.1039/c3ay41160e].

Ohno, T. 2002. Fluorescence inner-filtering correction for determining the humification index of dissolved organic matter. Environmental Science & Technology 36:742-46.

Pace, M. L., I. Reche, J. J. Cole, A. Fernandez-Barbero, I. P. Mazuecos, and Y. T. Prairie. 2012. pH change induces shifts in the size and light absorption of dissolved organic matter. Biogeochemistry 108:109-118 [doi:10.1007/s10533-011-9576-0].

Parker, C. A., and W. T. Rees. 1962. Fluorescence spectrometry—A reveiw. Analyst 87:83-111 [doi:10.1039/an9628700083].

Patel-Sorrentino, N., S. Mounier, and J. Y. Benaim. 2002. Excitation-emission fluorescence matrix to study pH influence on organic matter fluorescence in the Amazon basin rivers. Water Res. 36:2571-2581 [doi:10.1016/S0043-1354(01)00469-9].

Puchalski, M. M., M. J. Morra, and R. Vonwandruszka. 1991. Assessment of inner filter effect correction in fluorometry. Fres. J. Anal. Chem. 340:341-344 [doi:10.1007/BF00321578].

Senesi, N., T. M. Miano, M. R. Provenzano, and G. Brunetti. 1991. Characterization, differentiation, and classification of humic substances by fluorescence spectroscopy. Soil Sci. 152:259-271 [doi:10.1097/00010694-199110000-00004].

Sobek, S., L. J. Tranvik, Y. T. Prairie, P. Kortelainen, and J. J. Cole. 2007. Patterns and regulation of dissolved organic carbon: An analysis of 7,500 widely distributed lakes. Limnol. Oceanogr. 52:1208-1219 [doi:10.4319/lo.2007.52.3.1208].

Spencer, R. G. M., L. Bolton, and A. Baker. 2007. Freeze/thaw and pH effects on freshwater dissolved organic matter fluorescence and absorbance properties from a number of UK locations. Water Res. 41:2941-2950 [doi:10.1016/j.watres.2007.04.012].

Sun, F., W. S. Zong, R. T. Liu, J. Chai, and Y. Liu. 2010. Microenvironmental influences on the fluorescence of tryptophan. Spectroc. Acta A 76:142-145 [doi:10.1016/j.saa.2010.03.002].

Upstone, S. L. 2000. Ultraviolet/visible light absorption spectrophotometry in clinical chemistry. John Wiley & Sons Ltd.

Westerhoff, P., W. Chen, and M. Esparza. 2001. Fluorescence analysis of a standard fulvic acid and tertiary treated wastewater. J. Environ. Qual. 30:2037-2046 [doi:10.2134/jeq2001.2037].

White, A. 1959. Effect of pH on fluorescence of tyrosine, tryptophan and related compounds. J. Biochem. 71:217-220.

Zsolnay, A, E. Baigar, M. Jimenez, B. Steinweg, and F. Saccomandi. 1999. Differentiating with fluorescence spectroscopy the sources of dissolved organic matter in soils subjected to drying. Chemosphere 38:45-50.

Submitted 19 February 2013
Revised 16 October 2013
Accepted 6 November 2013